

IMPERIAL

IMPERIAL COLLEGE LONDON

DYSON SCHOOL OF DESIGN ENGINEERING

Development of a minimalistic actuation system for a novel pneumatic continuum robot

Design Engineering MEng - Master's Thesis

Author:

James Howells
CID: 01855361

Supervisors:

Dr. Nicolas Rojas
Dr. Thrishantha Nanayakkara

Submitted as part of the DE4 Master's Project. 7,691 words.

June 2024

Abstract—Soft robotics has potential to revolutionise robotics in certain applications. In particular, Pneumatic Soft Continuum Robots (PSCRs) show potential in mimicking dexterous biological movements such as an elephant’s trunk - however, the systems to actuate PSCRs are extremely expensive, or not optimised for the specific needs of the segments they control. Here, we propose a new pressure control system and corresponding actuation strategy tailored to the specific PSCR segments we develop. The segments represent an evolution of the STIFF-FLOP design, optimised for manufacture and made compatible with growing spines inserted into their centres to enable variable stiffness behaviours such as variable curvature. Three such segments are connected end-to-end, and a pressurisation system is built to control them. The system shows considerable potential: it uses segment parameters to speed up control, and has fewer, cheaper components than similarly-performing systems. These optimisations provide a 95% cost reduction compared to systems using commercial proportional pneumatic regulator valves. The robot and actuation system are incorporated into a stand-alone testing rig, which allows testing of other designs without tethers to external systems and is used to demonstrate the capabilities of the actuation strategy and compare PSCRs to rigid robots.

Contents

1	Introduction	1
1.1	Project Objectives	1
1.2	The Promise of Soft Robotics	1
1.3	Actuation Systems	2
1.4	Variable Curvature	2
1.5	Incentives for Accessibility	2
2	Segment Design	3
2.1	Segment Design Considerations	3
2.2	Selected Design: Fibre-Reinforced	3
2.3	Manufacturing Process	4
3	Actuation System	4
3.1	Supply System Requirements	4
3.2	Pump Capability	4
3.3	Pressure Control Algorithm	5
4	Results and Discussion	8
4.1	Segment	8
4.2	Pressure System with One Segment	9
4.3	Whole System Response	11
4.4	Physical Testing	12
4.5	Evaluation against Requirements	14
5	Conclusions and Further Work	14
5.1	Project Achievements	14
5.2	Further Work	15
5.3	Conclusions and Impact	15
References		15
6	Appendices	17

1 Introduction

1.1 Project Objectives

The overarching objectives of the work are to develop and evaluate a minimalistic actuation strategy for multi-segment pneumatic continuum robots, and to design and build a PSCR with which to test this actuation system. Present systems to provide soft robots with air pressure ('Actuation Systems') are not optimised for PSCRs, or are prohibitively expensive for many projects (see *1.3. Actuation Systems*). In order to tackle this, the following main objectives must be fulfilled:

1. Designing and building a minimalistic and cost-effective actuation system tailored to PSCR segments, and developing the actuation strategy to match.
2. Designing and building a new PSCR segment optimised for the addition of variable curvature mechanisms.
3. Bringing 1. and 2. together into a full 3-segment PSCR with a 3D workspace.
4. In addition, the design and manufacture of the segments must be made simple and accessible, to ensure that the work can easily be reproduced and further developed by others.

2. is required for testing of the actuation system: off-the-shelf PSCR segments do not exist, so these must be designed and built. The completed robot should also have a central lumen (cylindrical void) along its length so that it can additionally be used to test variable stiffness spines (or similar), inserted into its centre (see *1.4. Variable Curvature*). A 3-segment length is ideal because it provides a large, approximately-hemispherical workspace, and because its requirement for at least 9 separate pressure inputs provides a good test for the actuation system.*

1.2 The Promise of Soft Robotics

Soft robotics is a very promising field of research. Conventional robotics produces ever more capable robots, so the switch to researching less-developed soft alternatives can seem a counterintuitive – however, soft robots have the capability to transform robotics in certain applications. Conventional robots can, in some situations, pose a danger to their operators by their non-compliant nature, and there are some applications for which conventional robots are not well suited. For example, navigating in confined spaces or unstructured environments - such as the inside of a human body (for surgery [1]) or rubble in the aftermath of natural disasters (for search and rescue). These applications are ideally suited to soft robots.

*A PSCR segment needs at least 3 chambers to move in 3 dimensions - so a 3-segment robot requires at least 9.

PSCRs such as the one developed here are made of soft materials and possess theoretically infinite degrees of freedom as they can deform at any point within their soft continua [2]. Their segments are made of a soft silicone body with chambers inside: pressurising the chambers using an external air supply causes the segments to deform (they can bend, extend, contract, or otherwise change shape [3]). This principle can also be used in reverse: deforming the segments causes a change in pressure inside the chambers, which can be measured and used as a form of sensor [4]. The capabilities of a soft robot can be enhanced by connecting multiple, independently-controllable segments to each other – for example to produce longer arms [5] or even quadrupeds [6].

1.3 Actuation Systems

PSCRs require an external source of pressure to operate. The literature on existing pressure control systems is sparse: the focus for papers in soft robotics tends to be on segments themselves [7][8], or on ways to characterise and control them [9][10] – it tends to be taken as a given that systems exist to provide the required pressure. These systems do exist in several types, but each has its own issues. Perhaps the most common type uses a compressor connected to one Pneumatic Regulator per chamber [11]. These are capable of delivering pressure accurately, to within 1% [12], but come with the considerable cost of £430 per unit. This system, while accurate, costs over £1200 for the valves alone per 3-chamber segment – and requires a separate compressor. This may well be attainable for research projects but presents a major obstacle to the further development and adoption of PSCRs (as discussed in 1.5. *Incentives for Accessibility*).

A second type of pressure control system uses smaller DC pumps and simple valves to provide pressure – this has been used to great effect in versatile controllers such as FlowIO [13], which is designed to be the ‘Raspberry Pi of soft robotics.’ As such, it is extremely adaptable to different requirements but is not tailored to suit the needs of PSCRs. A similar concept has been used to create a system capable of supplying programmable positive or negative pressure to soft robotic segments [14], with more powerful pumps and better deflation control.

1.4 Variable Curvature

In current robots, each segment can have only one bending profile at a time, described by an arc radius R and an angle θ (Figure 1). This means each segment can have only one curvature at a time, which imposes fundamental limitations on PSCRs: for example, a PSCR cannot move like a snake (where the locus of the bend translates down the length of the animal [15]), and cannot achieve the dexterity and manipulation of, for example, an elephant’s trunk. The solution to this problem lies in variable curvature – where a single segment can have multiple bending profiles along

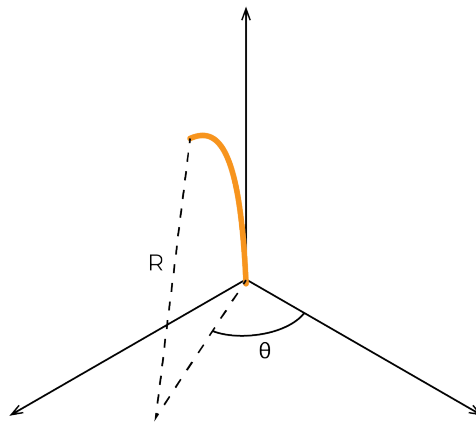


Figure 1: A single-curvature segment (orange) at some bending radius R and angle θ .

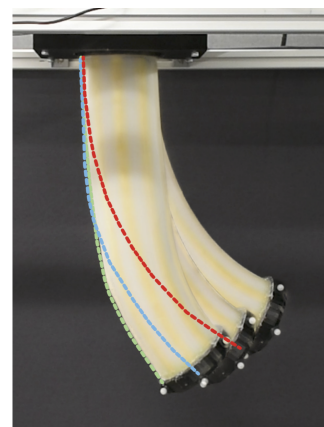


Figure 2: A variable curvature continuum segment – the first designed to be dynamically reconfigurable and continuous – showing various possible bending profiles. Figure courtesy of [7].

its length. Robots with a variable curvature capability are able to achieve precise motion and locomotion tasks that other types of robot cannot.

One of the only PSCRs capable of self-controlled variable curvature [7] uses a growing, jammable spine to lock the curvature of part of a segment, so the rest is free to take up a different profile (Figure 2). Other systems capable of variable curvature include tendon-driven robots [16] or ones using Shape Memory Alloys – but often these must be manually pre-configured to a single variable-curvature profile [17].

1.5 Incentives for Accessibility

Within research, accessibility refers to, ‘the ability of an individual to enter, navigate and comprehend’ a field [18]. In developing fields such as soft robotics, this is extremely important: it is vital that new researchers and hobbyists alike can get into the field and make valuable contributions to it. This helps accelerate development: many meaningful contributions to fields are made outside academia – for example one of the most-complete robotic imitations of a human hand, the open-source DexHand, was first developed by a single individual [19].

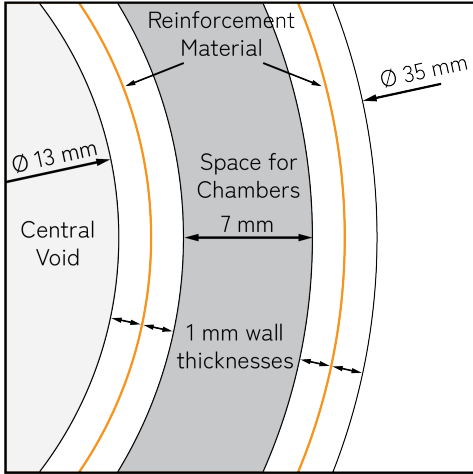


Figure 3: Section of a segment envelope, showing theoretical reinforcement zone (orange) and the space left for air chambers (dark grey). The final segment used circular cross-section chambers.

Excellent resources, such as the Soft Robotics Toolkit [20], do exist to help achieve this within soft robotics but they lack detailed guidance for PSCRs, and do not address the financial issues discussed above.

2 Segment Design

The first task was to design and produce a PSCR segment for testing. It had to be easy to manufacture, and feature a large central lumen to be compatible with inserted spines.

A PSCR segment contains airtight chambers arranged radially within a silicone cylinder, and pumping air into these chambers causes them to expand. A reinforcement material is used to constrain radial expansion, so the chambers can only get longer. Uneven extension between the multiple chambers then causes the segment to bend.

2.1 Segment Design Considerations

The segments were required to have a Ø13 mm lumen for insertion of growing spines, which significantly constrained their external diameter: the silicone casting process made producing walls of under 1 mm challenging, and these had to be cast on both sides of the reinforcement, so the chamber walls had to be at least 2 mm thick. In order to leave at least 7 mm for pressure chambers, a minimum overall diameter of 35 mm was selected (Figure 3).

Two different types of silicone were used for the segments: the relatively soft Smooth On[©] EcoflexTM 00-50, which gave the unpressurised segments little rigidity but made them very flexible, and the stiffer Dragon SkinTM 10 (also by Smooth On). The Dragon Skin segment wash chosen to provide rigidity and support to the base of the robot, while using Ecoflex for the middle and tip segment provided dexterity. The relatively

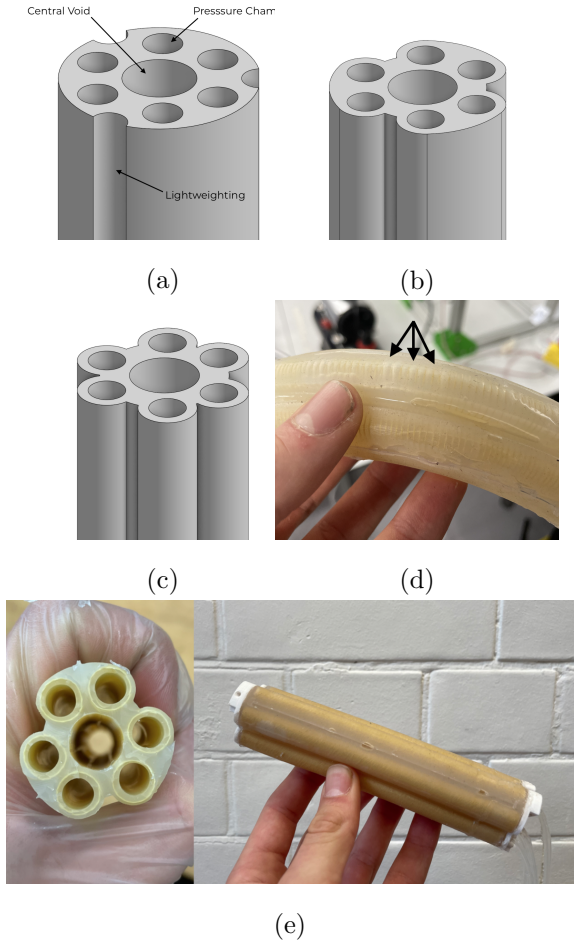


Figure 4: (a)-(c): Lightweighting strategies to reduce silicone use, from least to most aggressive. (b) was found to be optimal, since (c) removed so much material that segments lacked rigidity. (d): Ballooning between fibre reinforcing strands when strands were spaced too far apart. (e): The cross-section of a segment before the plugs were cast and end connectors glued on (left); a full segment with 3D-printed end connectors for joining segments together.

small diameter of the segments and the relatively soft silicones used meant that the robot would primarily be suitable for inspection and monitoring tasks, where the end effector would be a camera or sensor, rather than a manipulator.

2.2 Selected Design: Fibre-Reinforced

After investigating different segment geometries and reinforcing materials (see *Appendix B.1. Instant Segments*), a fibre-reinforced design with cylindrical chambers was selected. The design proposed represents a more compact evolution of the one used for variable curvature [7], in itself an evolution of the original STIFF-FLOP design [21]. Considerable developments have been made in simplifying the moulds and manufacturing process, increasing their repeatability and bringing them in line with the aim to make soft robotics more accessible.

The design had six chambers, each paired with their

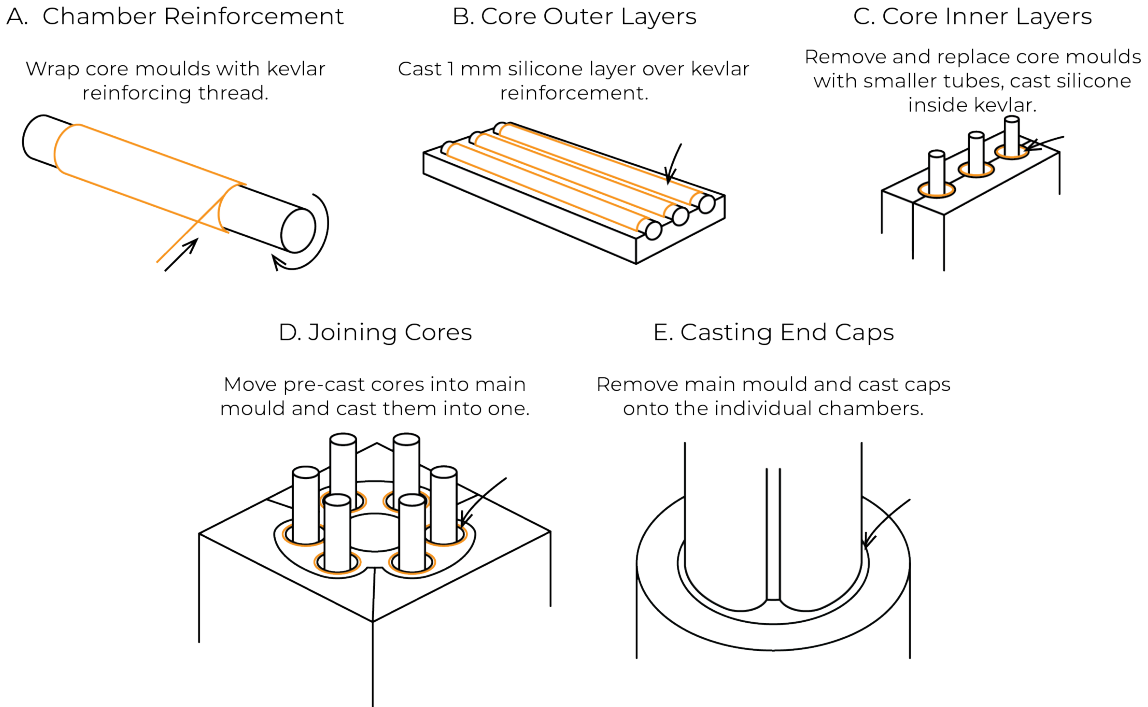


Figure 5: The five-step manufacturing process for making a segment: the first involves no silicone pours, and the last involves two but both are very simple. Detailed explanation has been made available at 3-pscr.github.io.

neighbour to form three zones (a connected pair of chambers) to enable bending in any direction. The chambers were circular and individually-reinforced, keeping diametrical change when pressurised minimal: this ensured that the diameters of the segment and the lumen were as constant as possible. The segments included optimised lightweighting to reduce unnecessary silicone use, and varying densities for the reinforcing fibres were investigated (Figure 4).

2.3 Manufacturing Process

Improved manufacturability of the segments when compared to previous designs was a key aim, so the moulds and casting process were carefully designed for speed and repeatability. Only a few off-the-shelf components were needed (7 mm OD and 9 mm OD brass tubes for the moulds - other mould components were printed). The only other parts required were the Kevlar fibres for reinforcement, and the chosen silicone to be cast.

Kevlar fibres were wound into reinforcing sleeves which were encased in silicone, before six reinforced chambers were cast into the finished segment. The end plugs could then be cast onto the ends to make the chambers airtight. The process is shown in Figure 5. To make the new segment design and manufacturing process as replicable as possible, the CAD has been made available online [22], and full documentation of the process and an accompanying video has been published [23].

Each segment required 5 separate silicone pours and took only a few hours of work, even including silicone cure times: a segment could be made in around 5 hours.

3 Actuation System

Once the segments were made, an air supply system and corresponding actuation strategy were needed to pressurise them.

3.1 Supply System Requirements

There were three hard requirements for the supply system: it had to provide a different pressure to each zone within the robot, the accuracy of the provided pressure had to be the same or better than the positional accuracy of the segments themselves (see 4.1.3. *Repeatability*), and the system had to be relatively inexpensive compared to previous solutions. In addition, it was desirable that the system be fast enough to pressurise a segment within two seconds and be relatively easy to build.

3.2 Pump Capability

At first, building a custom piston pump was investigated due to the cost savings this could offer (see Appendix B.2. *Piston Pump*). This was found to be ineffective, so small diaphragm pumps (which can be used to control PSCRs [14]) were selected instead. Three small DC pumps (XW-802s [24]), theoretically capable of supplying up to 300 kPa were used. Their pressure capability was tested without a segment attached (pressurising a blind section of tube), and was found to plateau at 94 kPa after 0.9 seconds (see Figure 6). This is considerably less than advertised, but nonetheless sufficient for the segments designed.

It was found that a command PWM duty cycle of

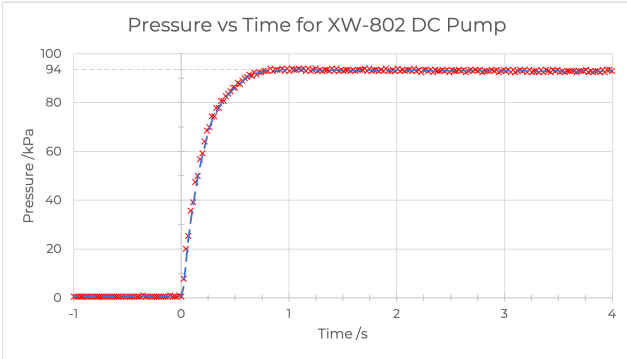


Figure 6: The DC pumps were able to achieve a maximum pressure of 94 kPa in approximately 0.9 seconds.

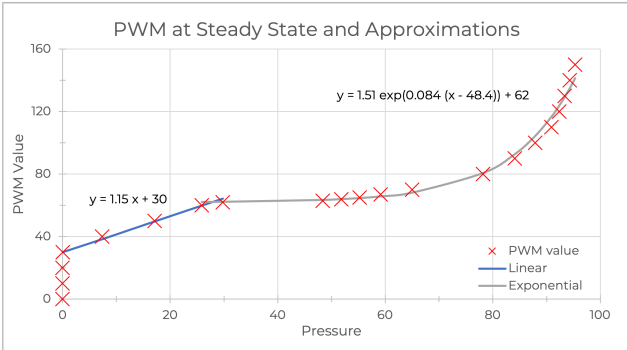


Figure 7: The chambers within a segment tended towards a steady state pressure when the pumps were run at a constant speed. Shown here is PWM value (0-255) at steady state pressure, with a linear and exponential phase.

60% (150 out of 255 on Arduino) was sufficient to reach the 94 kPa maximum - a higher duty cycle did not result in higher pressure. Lower duty cycles also had corresponding steady state pressures, and these steady states were linear with respect to PWM duty cycle below 28 kPa, and exponential for higher pressures (see Figure 7). The exponential section was likely caused by higher internal pressures of the segment making it respond less to small perturbations in pressure, and requiring more energy to work against the elastic effects of the silicone and increase air pressure further.

One fundamental limitation of the DC pumps was that they could not accurately control pressure when deflating the segments - air would rush through uncontrolled at any pump speed. In order to combat this, and reduce the number of pumps required from one per zone (as has been used previously [14]) to one per segment, each pump was connected to three zones via 5 low-cost solenoid valves - Figure 8. This meant that the overall cost of the hardware to control three zones was around £60 (including solenoid valves), or £180 for the whole 3-segment robot – a 95% reduction on solutions using pneumatic regulator valves. The system required only basic tools to build, and a 3D printer was helpful for making mounts for components but not essential.

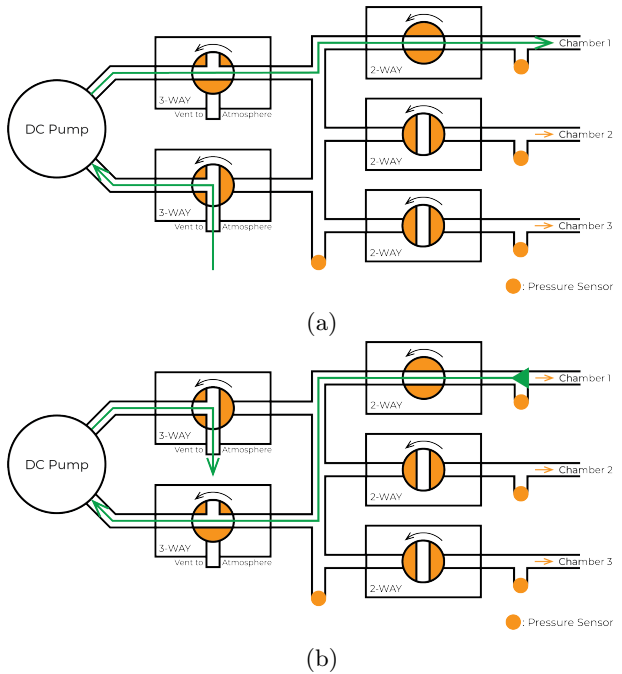


Figure 8: The solenoid valve setup in inflation mode for Chamber 1 (a), and deflation mode for the same chamber (b).

3.3 Pressure Control Algorithm

The pressure control algorithm to run this system was considerably more complex than similar algorithms because each pump controlled three separate zones to different pressures. The system ran on a single Arduino, and there were two key issues in designing the system: the control of the pumps to provide the required output pressure (*3.3.1. Inflation Control: Direct Mapping*), and solenoid valve control to achieve smooth lowering of pressure (*3.3.2. Creep Deflation*).

3.3.1 Inflation Control: Direct Mapping

In order to inflate zones by a controlled amount, PID control was initially implemented, but was found not to be the most effective approach: a direct mapping approach worked better. The mapping between PWM value and steady state pressure characterised in *3.2. Pump Capability* was implemented directly, where a target pressure could be converted to the needed PWM value by the following equation (to two significant figures):

$$\text{PWM} = \begin{cases} 1.2x + 30 & \text{for } x \leq 28 \\ 1.5e^{0.084x-48} + 62 & \text{for } x > 28 \end{cases}$$

where x is the target pressure. At steady state, this produced the correct pressure, but was found to be quite slow and, at low PWM values (< 50), the DC pumps did not spin at a consistent speed and thus did not produce a consistent pressure. In order to address these issues, a constant positive offset was added to the exponential phase (> 28 kPa), and the linear section was replaced by a constant:

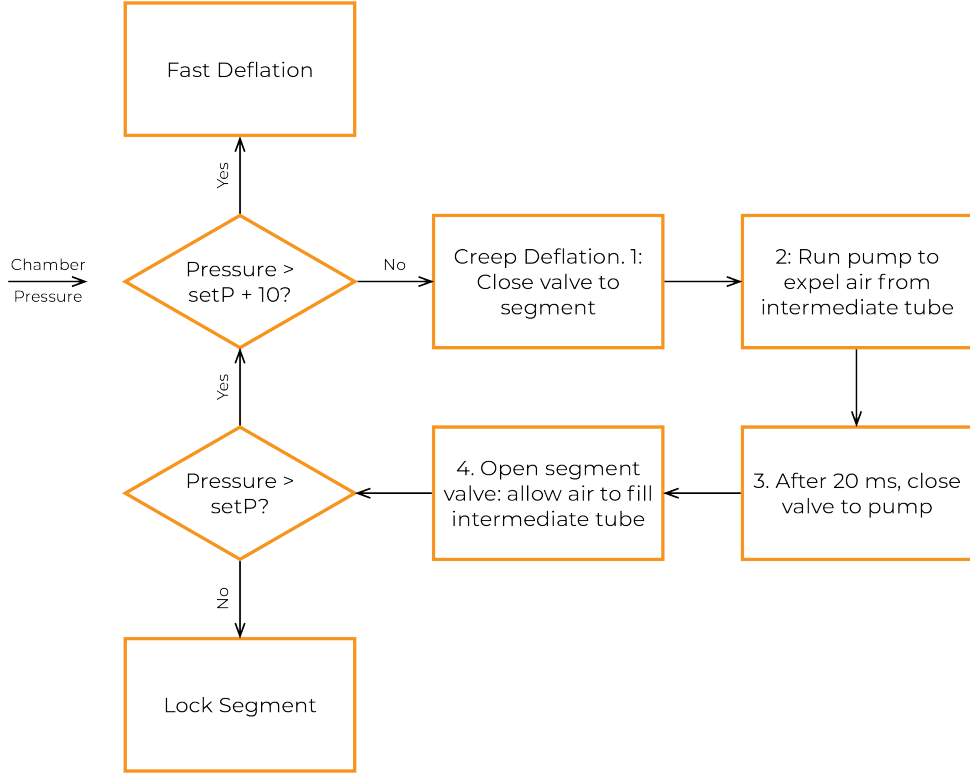


Figure 9: If chamber pressure is above set pressure, the above flow is used to reduce pressure. Rhombuses represent decisions, rectangles actions.

3.3.3 Actuation Strategy

$$\text{PWM} = \begin{cases} 82 & \text{for } x \leq 28 \\ 1.5e^{0.084x-48} + 82 & \text{for } x > 28 \end{cases}$$

This resulted in too high a pressure being produced, but this could be corrected by locking the chamber with the solenoid valves once the target pressure was reached. Using the PWM values produced by the equation (rather than a fixed, high duty cycle) ensured that the correct pressure was approached at a rate such that the program was able to lock the chamber before pressure rose too high. In addition, to correct for any steady state errors, a small integral error term was added to the controller that would slowly increase PWM duty cycle until required pressure was met.

3.3.2 Creep Deflation

Due to the aforementioned issues with depressurising segments, a ‘creep deflation’ mode (similar to the ‘slow pulsed deflation’ proposed by [14]) was implemented. This would be active when the current pressure was between 1.2 and 10 kPa more than the set pressure (above a 10-kPa difference full, uncontrolled deflation could be used).

Creep deflation involved using the section of pneumatic hose between a zone’s solenoid valve and the pump itself as a small pressure vessel to remove small amounts of air from the chamber with each cycle, as shown in Figure 9.

The Direct Mapping and Creep Deflation pressure control methods were built into a full control algorithm, the operation of which is shown in Figure 10. The system was able to use only 3 pumps to control 9 zones thanks to its actuation strategy, which involved queuing zones. Each pump would then work through its Pressurisation Queue until all of its zones were at the required pressure.

In addition to controlling the pressure of the segments, it was decided to add an extra degree of freedom to the robot: the base of the robot could be translated vertically by approximately 175 mm (Figure 11). This was actuated by a stepper motor driving a lead screw and was controlled directly by the Arduino.

3.3.4 Graphical Serial Interface

As the program grew in complexity, interfacing with it through Serial became unwieldy, so a simple graphical interface was built in Python. Communication with the board was in the form of a JSON-like string, sent over the Serial port. The Arduino supplied information on the status of each segment and the interface returned information on new set pressures and commands for the extra degree of freedom.

The resulting GUI (Figure 12) is lightweight and easily adaptable to other PSCRs with some simple changes to the layout of the interface, and is made available through GitHub [25].

PSCR Pressure Control Algorithm Structure

For every chamber in the robot:

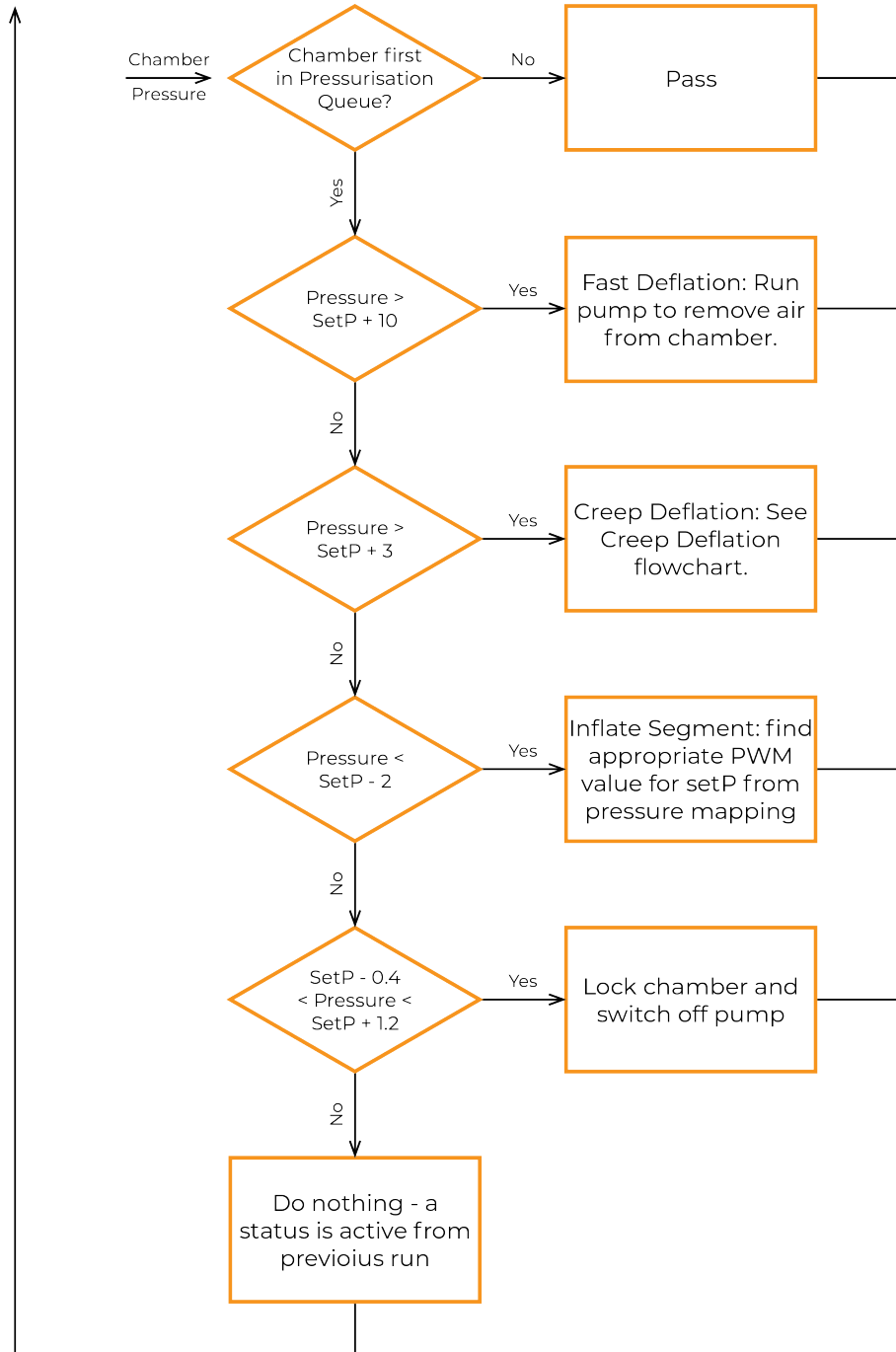


Figure 10: The logic the system used to control the pressure of individual chambers. The algorithm had separate lock (see 4.1.3. *Repeatability*) and unlock conditions, meaning that the system was less sensitive to small perturbations. For the creep deflation logic, see Figure 9. Rhombuses represent decisions, rectangles actions.

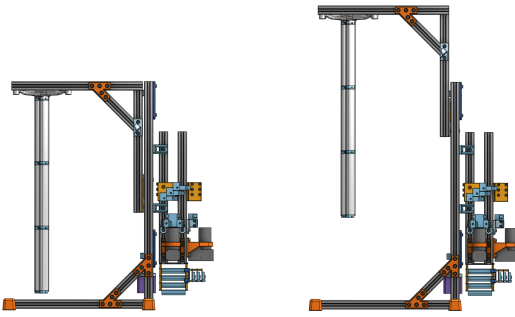


Figure 11: The whole rig in the home position (left) and with the extra Degree of Freedom extended upwards. It offered 175 mm of travel to greatly improve the workspace of the arm.

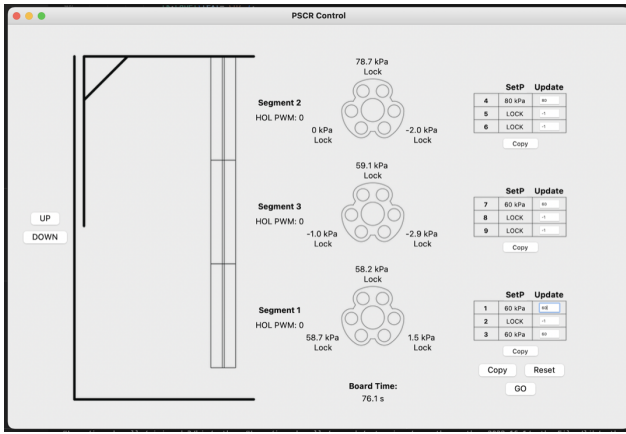


Figure 12: The simple GUI built in Python and Tkinter for controlling the three-segment PSCR. It communicated with Arduino over Serial.

4 Results and Discussion

Once each of the subsystems (*2. Segment Design*, *3. Actuation System* and *3.3. Pressure Control Algorithm*) had been created, they were tested and evaluated individually before being assembled and tested together.

4.1 Segment

4.1.1 Manufacturing Process Results

The new process made segments considerably more consistent. By optimising the way individual pours were carried out, it only had one critical pour (the second, when the inside walls of the chambers are being cast): small imperfections in each of the other pours could be corrected later, without having to start from scratch. The 5-hour manufacture time was a considerable improvement compared to before the mould was optimised, when manufacture of a single segment took up to one week with multiple pours failing and having to be restarted.

One remaining issue, however, was delamination. In a small proportion of the segments, the outer silicone sheath would not adhere properly to the Kevlar fila-

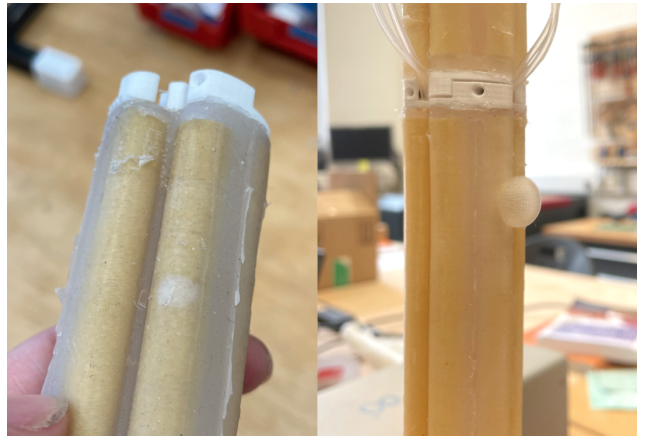


Figure 13: Delamination (left) and ballooning in segments, caused by imperfections in the bond between silicone and Kevlar, and in the inner core cast respectively.

ments. In most cases, this caused no issues – however, where delamination aligned with an imperfection in the inner walls, this resulted in ballooning (Figure 13). Of the total of 60 chambers manufactured for 10 segments, this only happened in one chamber. Increasing the distance between the Kevlar filaments was found to eliminate delamination, but in itself created more ballooning (Figure 4d).

4.1.2 Direct Air Pressure Response

In order to characterise pressure response of the segments across varying pressures, the pressure supply system was locked to provide a fixed pressure. This pressure was recorded, along with an image of the actuated segment and a scale bar on the same plane (to reduce parallax, Figure 14). Pixel-coordinates of the base and tip of the segment could be measured off the images, and the scale bar and some basic trigonometry were used to calculate the bend radius of the segment. As is standard in the characterisation of continuum robot segments [26], this was converted to a curvature value ($k = 1/R$), which ensures that more-curved segments have *higher* rather than lower characteristic values. The results, comparing the EcoFlex 00-50 and Dragon Skin 10 segments, are presented in Figure 15.

These results strongly suggest that the curvature for both types of silicone is related to supplied pressure by linear equations. Both suggest an intercept at $(0, 0)$ as expected: there is no curvature at atmospheric pressure.

The relationship between pressure and bend *radius*, however, is a decreasing exponential: the higher the pressure, the more extra pressure needed per unit decrease in radius. This fits well with the stress-strain curve of hyperelastic silicones (Figure 16): the relationship between deformation (strain) and applied pressure (force / area, stress) is nonlinear, with high deformations (in this case, low bend radii) requiring disproportionately more pressure than lower ones.



Figure 14: A Dragon Skin 10 segment at 80 kPa, with a ruler in plane with the segment being used as a scale bar to calibrate measurements taken from the image.

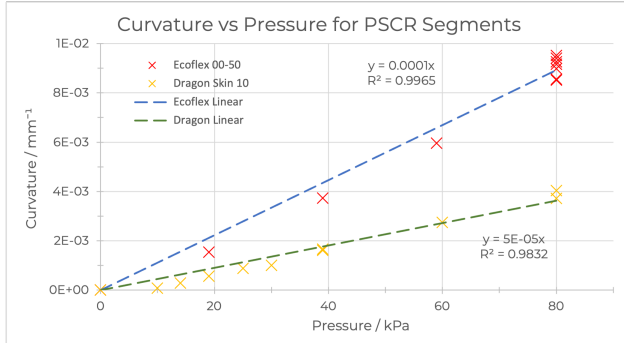


Figure 15: The relationships between supplied pressure and segment curvature were found closely to follow linear equations, with intercepts at the origin: no pressure means no curvature.

4.1.3 Repeatability

It was important to characterise the positional accuracy of the segments for a given pressure, because there is little point in making an actuation system that is more accurate than the segments themselves (and conversely pressure control systems less accurate than the segments waste segment capability on pneumatic uncertainty).

Repeatability was tested at the segments' maximum design pressure, because this yielded least uncertainty (a more rigid segment is less susceptible to small changes in air pressure or external stimuli). This meant that the repeatability was characterised in the 'best-case' scenario, which would require the highest accuracy from the pressure control system - the segments would not get more precise than this. Each segment was repeatedly cycled from 0 to 80 and back to

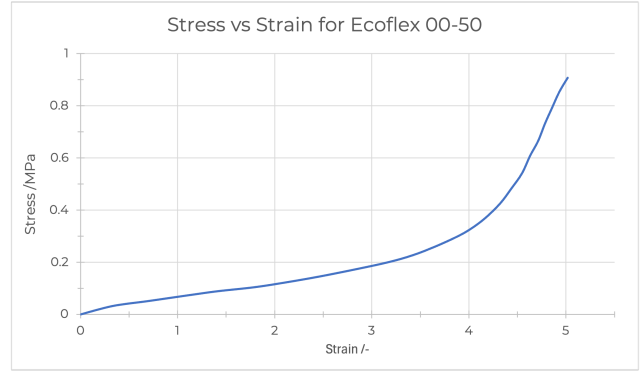


Figure 16: Stress vs Strain for Ecoflex 00-50: as with many elastic materials, the response is nonlinear and high deformations require more stress per strain [27].

0 kPa, with the position at 80 kPa being captured. Measurement of the pressure relied on the pressure sensors, which were susceptible to noise, so long-run averages were used to correct for this. The results are displayed in Table 1. The total uncertainty in curvature for Ecoflex was found to be 11%, and for Dragon Skin 19% - but, especially for the Dragon Skin, the lowest-curvature result seemed anomalous.

Run Number	Bend Radius / mm		Curvature / mm^{-1}	
	EcoFlex	Dragon Skin	EcoFlex	Dragon Skin
1	117	206	8.6e-3	4.9e-3
2	111	204	9.0e-3	4.9e-3
3	109	204	9.2e-3	5.0e-3
4	108	201	9.3e-3	5.0e-3
5	106	201	9.4e-3	5.0e-3

Table 1: Repeatability of radius and curvature ($= 1/\text{radius}$) for Ecoflex and Dragon Skin segments at 80 kPa, ordered straightest to most curved. Ecoflex segments' curvature was slightly under double that of Dragon Skin ones.

With anomalies excluded, the Ecoflex had a variability of 9%, and Dragon Skin 2% - i.e. a pressure control system cannot achieve positional accuracy of better than $\pm 4.5\%$ (Ecoflex) / $\pm 1\%$ (Dragon Skin) without feedback. The difference between the two silicones is likely due to the elastic effects already discussed: when the segments are more rigid (either due to greater air pressure or because of the silicone they are made out of), they are less susceptible to small changes in air pressure or other external perturbations, and are thus more positionally accurate.

4.2 Pressure System with One Segment

The pressure control system (Figure 17) could supply up to 87 kPa (2 s.f.) independently to up to 9 zones. This was in line with the 80 kPa design pressure of the segments, but slightly lower than the pump capability of 94 kPa (see 3.2. *Pump Capability*): maximum pressure could likely be improved with larger-diameter tubing or less constricting solenoid valves (Figure 18). In order to evaluate the pump against its original aims, it

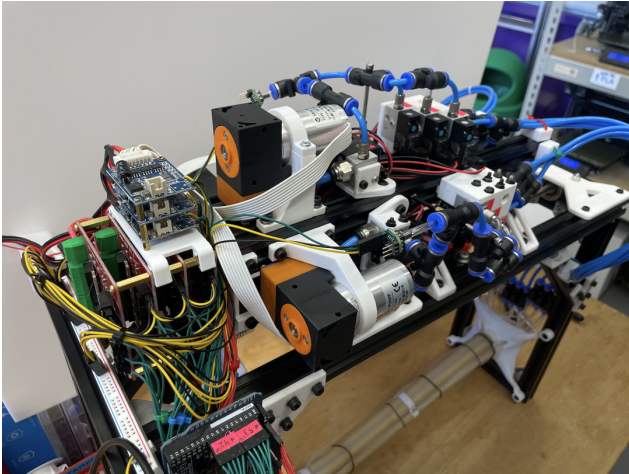


Figure 17: The pressurisation system as built, with its three pumps and fifteen solenoid valves controlled by a single Arduino Mega.

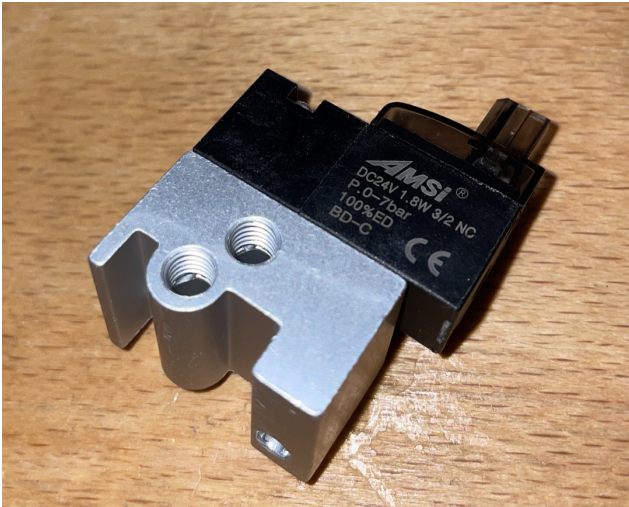


Figure 18: The solenoid valves had very small holes connecting the ports - just visible at the base of the threads. This is likely to have constricted airflow significantly.

was connected to a single segment and a pre-set Pressure Cycle was used (the robot stepped through an array of pressures, holding each pose for 0.5 s before moving on, Figure 19).

4.2.1 Pressurisation Time

Pressurising a zone from atmospheric pressure to 80 kPa took around 3 seconds for segments made of both silicones (Figure 20). This is 50% slower than the targeted 2 s. The cause of this was found to be the pumps themselves: according to their datasheet, they were able to supply 180 - 450 ml min⁻¹. Given the optimism of the datasheet on maximum pressure (94 kPa reality vs 300 kPa stated), the lower bound was taken. The volume of a zone was 10,780 mm³ (see Appendix B.2. *Piston Pump*), which suggests a pressurisation time of 2.87 s - very close to the observed 3 seconds. Increasing the PWM duty cycle sent to the pumps above the val-

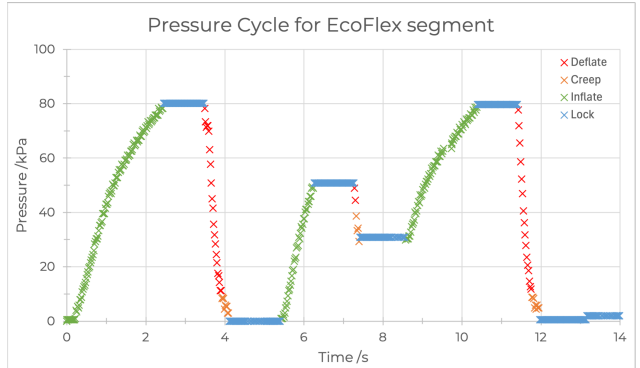


Figure 19: An Ecoflex segment running a Pressure Cycle: the system is able to reach all target pressures within range, smoothly.

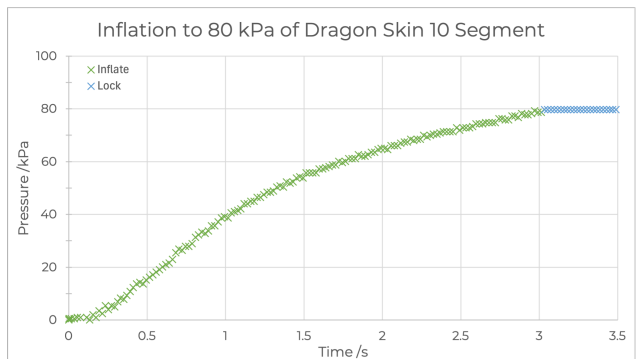


Figure 20: A Dragon Skin segment being inflated to 80 kPa: inflation takes almost exactly three seconds - 50% slower than target.

ues suggested by the direct mapping (*3.3.1. Inflation Control: Direct Mapping*) did not have any effect in speeding pressurisation up, again suggesting that the pumps were already working at or near capacity. This suggested that replacing the pumps would solve this issue - but pressurisation time is not critical, so this was not investigated further.

4.2.2 Accuracy

A key objective for the pressure control system was that its accuracy should be tailored to the segments: supplying pressure more accurately than the segments could replicate a pose had little benefit. As discovered in *4.1.3. Repeatability*, the lowest positional error that could be expected from a segment was around 2%, so the supply system had to be able to provide 2% accuracy. After tuning, a window of +1.5%/-0.5% at 80 kPa (+1.2, -0.4 kPa) was implemented: if a zone's pressure was within this window with respect to target pressure, the system would not attempt to correct it. This allowed the algorithm to achieve a pressure lock quickly. Biasing the window above the set pressure compensated for the small amount of air lost when closing the solenoid valves themselves, usually resulting in a pressure accurate to the nearest integer.

This window not only made sure that the system achieved pressure accurate enough for the segment, but



Figure 21: Creep deflation allowed the algorithm to drop segment pressure rapidly until close to the set pressure, then creep down to the target slowly with minimal overshooting. As can be seen here it was primarily required at higher target pressures.

also made the pressure control considerably less jittery: it meant that the controller was less susceptible to errors from the pressure sensors (which produced random noise of approximately ± 0.3 kPa[†]), pressure variations caused by the segments swinging, or the pressurisation of neighbouring zones subtly changing a zone's pressure. The result of this was smooth control of individual segments, with minimal overshooting and positive locking[‡] of segments once they had reached the correct pressure (Figure 19).

4.2.3 Creep Deflation Performance

The creep deflation algorithm was found to be very effective at reducing pressure in a controlled way. Unsurprisingly, the amount each creep deflation cycle reduced the pressure by was highly dependent on the starting pressure, with pressure dropping faster when pressure was higher: -3 kPa per cycle at 60 kPa, down to around -0.5 kPa at low pressures. Figure 21 shows a Pressure Cycle both with and without creep deflation: without creep deflation, pressure was likely to overshoot the set point - which then required subsequent inflation, wasting time.

4.3 Whole System Response

With the individual subsystems working well, the whole rig was assembled with its three segments, extra vertical degree of freedom, and pressure control system (Figure 22).

4.3.1 Interference between Zones

One potential issue with connecting multiple segments together was interference between zones: a movement of one segment could set the arm swinging, causing the pressures in other segments to fluctuate and creating instability in the controller as it tried to correct.

[†]Moving average filters were found to be ineffective at countering this, as they invariably caused pressure overshoots.

[‡]I.e. once locked, the zone does not leak and does not need to be unlocked until a new pressure is supplied.

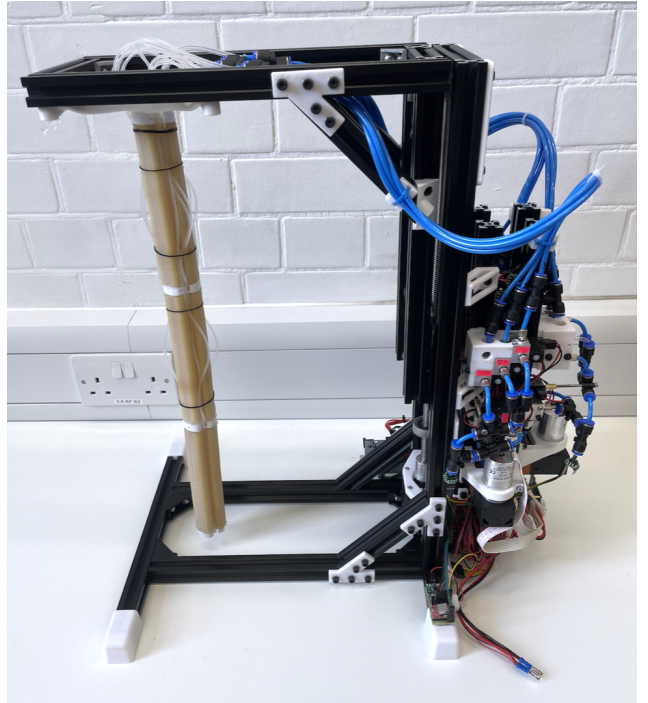


Figure 22: The whole system in one: the actuation system on the back of the rig (right), with the arm hanging from the movable platform.

When the arm was deliberately set swinging, it was found that the pressure variation this caused was significant (up to 3.5 kPa) and that segments nearer the top had more pressure variation (see Figure 23) because they deformed more when the arm was swinging. When pressure control was active, however, this effect was much less noticeable - and swinging caused far less noticeable variation in pressurised segments.

4.3.2 Dynamic Pressure Response

In order to assess the performance of the whole system in a repeatable way, Pressure Cycles were again used (*4.2. Pressure System with One Segment*). This allowed for direct comparison of different zones,

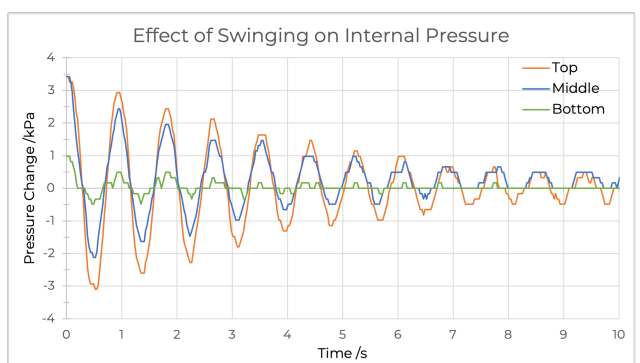


Figure 23: Oscillation-induced pressure variation as the arm swings: it was higher for the top segments, with an overall maximum of 3.42 kPa. With the system switched off, as here, oscillation was slow to die down.

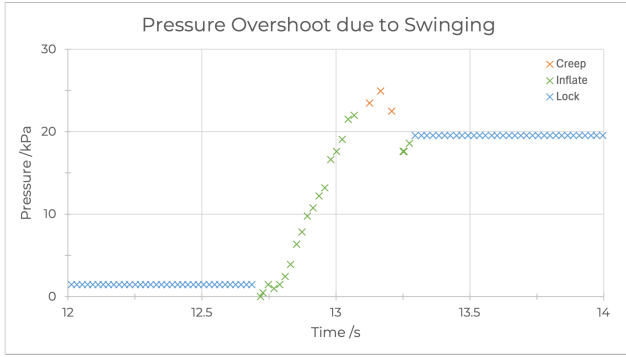


Figure 24: Pressure in a zone could overshoot the target in some cases, due to the pressure variations caused by the segment swinging.

chambers and separate runs against each other so that the effects of external factors could also be investigated.

Individual Segments

The segments in the robot were first tested one at a time. Each completed the Pressure Cycle with no major issues, however, one small anomaly was noted in the topmost segment. In the final stage of the Pressure Cycle (pressurising to 20 kPa), pressure overshot the set point by 4.9 kPa (Figure 24). The duration of the overshoot and subsequent undershoot closely matched the time period of oscillation of the whole arm, suggesting that it was partly caused by swinging of the whole robot.

It is logical that this anomaly only manifested itself in the final step of the Pressure Cycle because the previous steps were what caused the robot to swing in the first place, and it is reassuring to note that the swinging caused no issues despite pressure variation being significant (the overshoot was corrected by three creep deflation cycles in less than 0.1 seconds).

Multiple Segment Interactions

Multiple-segment interactions were investigated, using the same Pressure Cycle as used for individual segments but this time pressurising one zone per segment to the same pressure, and only moving on once all three zones had reached their targets.

The first notable change was the controller frequency: when controlling only one zone, the algorithm ran at 45.5 Hz (3 s.f.), but when all 9 zones were controlled, frequency dropped to 18.6 Hz. Later, when control was switched from a Pressure Cycle to the full program interfacing with the GUI, this dropped again to 4.30 Hz because of the time taken to read and write to the serial port. This made the system too unresponsive and led to overshooting, so the Serial communication had to be optimised: this managed to bring the frequency back up to 11.8 Hz and resolved the issue.

Actuating multiple zones led to a less smooth pressure response with more overshooting, as expected from the swinging dynamics above. However, because the Pressure Cycle aligned periods of pressure adjustment and non-adjustment (all zones were being

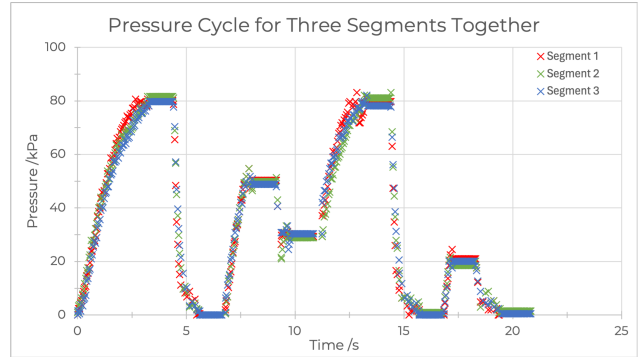


Figure 25: Despite movement-induced swinging in the arm, the control system is still able to achieve relatively smooth control, even when multiple segments are controlled at once.

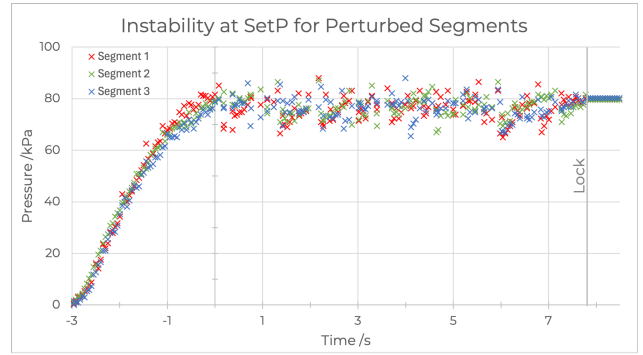


Figure 26: Small perturbations at the end effector could cause the arm significant difficulty in achieving a pressure lock, due to the pressure of one zone affecting its neighbours.

pressurised and then locked at approximately the same time), the swinging did not affect steady-state response: once the swinging was suppressed, ability of the arm to hold a pose was unaffected (Figure 25).

External Stimuli

External stimuli played a significant role in the pressure response of the whole system. Figure 25 was recorded with no external stimuli on the end effector, and runs where a constant pressure was applied to the end effector (slightly damping the swinging) had similar results. However, runs where slight, *variable* forces were applied to the end effector were found to be considerably less stable, with the system taking over 7 seconds (in extreme cases) to lock all chambers once target pressure had been reached (Figure 26). This would not cause problems for inspection tasks, but may need to be addressed for manipulation of complex objects.

4.4 Physical Testing

Basic demonstration rigs were built to test the capability of the actuation strategy and segments. In addition, tests were conducted to evaluate the performance of a soft robot against a similarly-sized conventional robot: a baseline 3-segment rigid robot was built, with 3D

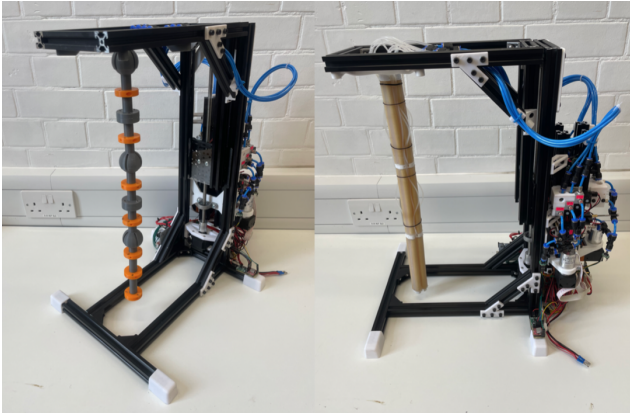


Figure 27: A basic dummy rigid robot (left) was created to test the PSCR against. The ball-and-socket joints were fully passive but allowed a high range of motion. Orange rings on the dummy simulate the thickness of the actual robot, in order to make the comparison a fair one.



Figure 29: With less than one segment protruding below the bottom of the fourth wall, the rigid robot was hardly able to move - but the PSCR was able to navigate out of the obstacle with ease.



Figure 28: The three-sided plywood obstacle with a fourth, transparent side extending only partway down it.

printed ball-and-socket joints and fully passive actuation: Figure 27.

4.4.1 Narrow Tunnel Obstacle

Soft robots are particularly suited to navigation in confined spaces or unstructured environments (see 1.2. *The Promise of Soft Robotics*). A simple obstacle was built to test this: a three-sided, square-section tunnel (55 mm square), with a fourth wall extending a quarter of the way down from the top (Figure 28). The robot was required to reach down inside the obstacle, and exit through the gap on the fourth side.

Single Segment

The soft robot found this an easy task, even when less than one segment was below the bottom of the fourth wall: the compliant nature of the robot and its curved actuation profile meant that fractions of the

first segment could protrude from the tunnel. In addition, once actuated, the single segment could bend laterally as well, further increasing its workspace.

By contrast, a traditional robot (even the hyper-dexterous ball-and-socket dummy created) could not exit the tunnel at all with any less than one segment below the bottom of the fourth wall (Figure 29).

Multiple Segments

With more than one segment protruding below the front wall of the obstacle, the rigid robot performed slightly better: the first segment could get out of the obstacle, and had some limited side-to-side motion. However, once again, the PSCR outperformed it quite considerably: because the segments themselves bend, it was able to wrap itself around the outside of the obstacle (Figure 30), which gave it an inspection reach very significantly better than what a rigid robot could achieve without at least three segments protruding. Actuation strategy became very important for this: an incorrect order of the Pressurisation Queue resulted in the robot trying to wrap around the obstacle before it had exited the channel, so it became jammed inside until it was depressurised.

4.4.2 Narrow Tunnel with Exit Hole

An evolution on the narrow tunnel was created, to give the PSCR more of a challenge and test how the extra translational degree of freedom (Figure 11) improved the capability of the robot. Instead of the fourth side of the obstacle being completely open other than the top quarter, an extra wall was added so that there was an opening of 55 mm square for the robot to pass through, 100 mm from the top of the obstacle. The rigid robot was entirely unable to pass through this opening.[§]

[§]It was even impossible to disassemble the robot and then re-assemble it passed through the opening: the maximum joint bending angle would not allow this.

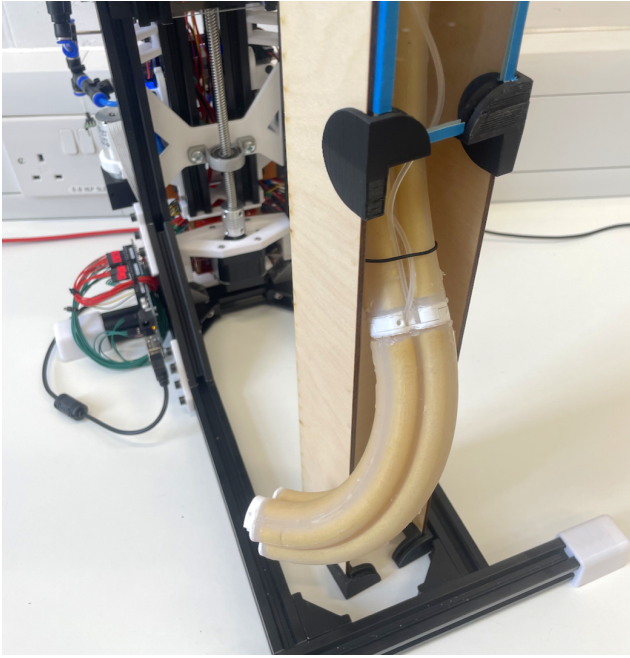


Figure 30: More than one segment protruding below the bottom of the fourth side allowed the PSCR to fully exit the obstacle to perform inspection tasks or similar. Once again, the rigid robot had a far more limited workspace.

Once again, the PCSR preformed well. The extra degree of freedom was used to raise the robot until the tip was just above the bottom of the exit hole, the segment was partially bent, and then the robot was moved down. This was repeated until the entire final segment, and part of the middle segment, protruded through the opening (Figure 31). Once again, the sections of the robot protruding through the opening could then wrap around the outside of the obstacle. This would only be possible for a rigid robot with extremely short segments, approaching a continuum - but this would be extremely challenging to drive, with each segment requiring several actuators.

4.5 Evaluation against Requirements

Once the segments and actuation system had been tested, they were evaluated against their original aims:

The **Segment** succeeded in its aim to be easy to manufacture, significantly cutting manufacture time - and the central Ø13 mm lumen was shown to be compatible with growing spines: a project running in parallel used the segment design to test variable stiffness mechanisms.

All three of the hard requirements for the **Actuation System** were fulfilled. Of the two desirable outcomes, the pressurisation time target of 2 seconds was not met - however, it was validated that this only affected the robot's speed, not its dexterity or its workspace.



Figure 31: When the fourth side was modified to have a small opening, the rigid robot was unable to exit the obstacle at all - however, because of its compliance, the PSCR was able to navigate through the hole and lower one and a half segments through it.

5 Conclusions and Further Work

5.1 Project Achievements

This project has used novel concepts to make improvements to PSCR systems: a new, minimalistic actuation system has been developed and tested, tailored to a specific PSCR segment type proposed.

5.1.1 Segments

A new segment design has been proposed, representing an evolution on the widespread STIFF-FLOP design [21]. It has been modified to include a larger central lumen, making it compatible with variable stiffness mechanisms currently gathering pace in soft robotics, and a set of moulds have been developed with corresponding documentation to speed up and simplify the manufacturing process and make the design available to other projects. Manufacturing time is around 5 hours, and maximum design pressure of the segments is 80 kPa.

5.1.2 Pressure Control System

A new actuation system has been developed to provide programmable pressure to each of the 9 independent zones of a 3-segment robot. Thanks to its novel actuation strategy (see 5.1.3. *Actuation Strategy*), the system uses fewer pumps than other comparable systems [14] and removes the need for expensive proportional regulator valves and compressors entirely – cutting costs by up to 95% compared to these systems. It can pressurise zones up to 87 kPa in 3 seconds – which is slower than targeted, but this does not impact the completed robot’s capabilities for inspection

and monitoring tasks. 3 seconds represents the limit of the pumps' capability, so decreasing this would likely involve using more capable (and thus costly) pumps.

5.1.3 Actuation Strategy

The modifications to the pressure control system were enabled by a new actuation strategy which could control more than one zone with each pump. This allowed 1/3 the number of pumps to be used compared to previous systems and was achieved by using a Pressurisation Queue: each zone that was not at the correct target pressure was added to a queue to be pressurised as soon as the pump connected to it became available. The resulting algorithm, built to run on an Arduino and control all of the pumps and solenoids needed for a three-segment PSCR, was tuned using information about the segments themselves to be accurate to 2% - the highest accuracy the segments were able to achieve.

5.2 Further Work

These developments do leave room for further work in a few specific areas: the new PSCR segment shows potential in terms of manufacturability, ease of control (80 kPa design pressure is relatively low) and dexterity, but more analysis of its capability is needed to build up a robust mathematical model of its behaviour and to better understand the dynamics between neighbouring zones. In addition, the new actuation strategy opens up opportunities for investigation into Pressurisation Queue ordering strategies: currently, the order of pressurisation is determined by a pre-set list – but, as discovered in 4.4.1. *Narrow Tunnel Obstacle*, the order of pressurisation can be significant, and there may be scope to implement forward-kinematic models which use ordering of the queue to achieve motion profiles that would otherwise not be possible. This, too, would require mathematical modelling of the segments, towards which detailed motion tracking studies of segment behaviour would need to be carried out.

In addition, further experimentation could be done in the casting process: the process proposed is successful at creating consistent segments relatively quickly, but it may be possible to remove one pour from the process, bringing the total number of pours down to four and saving up to an hour per segment cast.

5.3 Conclusions and Impact

In conclusion, the three-segment PSCR proposed, with its new actuation system and strategy, is well-suited to inspection and monitoring tasks due to its softness, compliance, and relatively small diameter. It has good dexterity and a large workspace owing to its three segments and extra translational degree of freedom, enabling it to navigate cramped environments that rigid robots would find very challenging. It contributes a new segment design with corresponding manufacturing process and set of moulds to the field, and these have been made freely available online to help lower the

barriers to entry in pneumatic soft continuum robotics. In addition, the novel, minimalistic actuation system provides pressure for PSCRs, to an accuracy tuned to the segments themselves and using cheaper components and fewer pumps than previous solutions. The robot and corresponding systems are housed on a modular, self-contained rig, with potential to be used as a standalone testing platform for further developments in segment design or pressure control systems. The new segment design's compatibility with central spines (owing to the 13 mm lumen down its centre), allows it to be used as a versatile test segment for variable stiffness and variable curvature systems – a purpose for which it is already being used.

Some optimisations do remain in the pressure control system, increasing its maximum output pressure and decreasing the time it takes to pressurise a zone, as well as implementing ordering of the Pressurisation Queue, but these do not interfere with the functioning of the system, which is robust and reliable.

Acknowledgements

This project would not have been possible without the input and support of my supervisors, Nicolas Rojas and Thrishantha Nanayakkara, and their REDS and Morph Labs at the Dyson School of Design Engineering at Imperial College London. Special thanks to Xinran Wang, who provided his time, expertise and continued guidance, and to Isaac Winson-Bushby for his work to create a welcoming workshop environment in the IDEAS Lab, without whose contributions this project would not have been possible.

References

- [1] Runciman M, Darzi A, Mylonas GP. Soft Robotics in Minimally Invasive Surgery. *Soft Robotics*. 2019;8(4):423-43.
- [2] Wang J, Chortos A. Control Strategies for Soft Robot Systems. *Advanced Intelligent Systems*. 2022;5(4).
- [3] Xavier MS, Tawk CD, Zolfagharian A, Pinskier J, Howard D, Young T, et al. Soft Pneumatic Actuators: A Review of Design, Fabrication, Modeling, Sensing, Control and Applications. *IEEE Access*. 2022;10:59442-85.
- [4] Leith A. Pneumatic Deformation Sensors; 2016. Available from: <https://softroboticstoolkit.com/pds>.
- [5] Katschmann RK, Santina CD, Toshimitsu Y, Bicchi A, Rus D. Dynamic Motion Control of Multi-Segment Soft Robots Using Piecewise Constant Curvature Matched with an Augmented Rigid Body Model. In: 2019 2nd IEEE International Conference on Soft Robotics (RoboSoft). IEEE; 2019. p. 454-61.

- [6] Drotman D, Jadhav S, Sharp D, Chan C, Tolley MT. Electronics-free pneumatic circuits for controlling soft-legged robots. *Science Robotics*. 2021;6(51).
- [7] Wang X, Lu Q, Lee D, Gan Z, Rojas N. A Soft Continuum Robot With Self-Controllable Variable Curvature. *IEEE Robotics and Automation Letters*. 2024;3;9(3):2016-23.
- [8] Zhang J, Liu L, Chen Y, Zhu M, Tang L, Tang C, et al. Fiber-reinforced soft polymeric manipulator with smart motion scaling and stiffness tunability. *Cell Reports Physical Science*. 2021;10;2(10):100600.
- [9] Polygerinos P, Wang Z, Overvelde JTB, Galloway KC, Wood RJ, Bertoldi K, et al. Modeling of Soft Fiber-Reinforced Bending Actuators. *IEEE Transactions on Robotics*. 2015;6;31(3):778-89.
- [10] Katzschatmann RK, Santina CD, Toshimitsu Y, Bicchi A, Rus D. Dynamic Motion Control of Multi-Segment Soft Robots Using Piecewise Constant Curvature Matched with an Augmented Rigid Body Model. In: 2019 2nd IEEE International Conference on Soft Robotics (RoboSoft). IEEE; 2019. p. 454-61.
- [11] Booth JW, Case JC, White EL, Shah DS, Kramer-Bottiglio R. An addressable pneumatic regulator for distributed control of soft robots. In: 2018 IEEE International Conference on Soft Robotics (RoboSoft). IEEE; 2018. p. 25-30.
- [12] Electro-Pneumatic Regulator Series ITV1000;. Available from: <https://docs.rs-online.com/bbe6/0900766b813f0f69.pdf>.
- [13] Shtarbanov A. FlowIO Development Platform – the Pneumatic “Raspberry Pi” for Soft Robotics. In: Extended Abstracts of the 2021 CHI Conference on Human Factors in Computing Systems. New York, NY, USA: ACM; 2021. p. 1-6.
- [14] Zhang B, Chen J, Ma X, Wu Y, Zhang X, Liao H. Pneumatic System Capable of Supplying Programmable Pressure States for Soft Robots. *Soft Robotics*. 2022;10;9(5):1001-13.
- [15] Jayne BC. Kinematics of Terrestrial Snake Locomotion. *Copeia*. 1986;12;1986(4):915.
- [16] Pogue C, Rao P, Peyron Q, Kim J, Burgner-Kahrs J, Diller E. Multiple Curvatures in a Tendon-Driven Continuum Robot Using a Novel Magnetic Locking Mechanism. In: 2022 IEEE/RSJ International Conference on Intelligent Robots and Systems (IROS). IEEE; 2022. p. 472-9.
- [17] Wang P, Guo S, Wang X, Wu Y. Design and Analysis of a Novel Variable Stiffness Continuum Robot With Built-in Winding-Styled Ropes. *IEEE Robotics and Automation Letters*. 2022;7;7(3):6375-82.
- [18] Harniss M. Accessibility. In: Encyclopedia of Quality of Life and Well-Being Research. Dordrecht: Springer Netherlands; 2014. p. 9-10.
- [19] Rob Knight. DexHand;. Available from: <https://www.dexhand.org>.
- [20] Bira N, Walsh C, Grupper J, Golecki H. Soft Robotics Toolkit;. Available from: <https://softroboticstoolkit.com/>.
- [21] Cianchetti M, Ranzani T, Gerboni G, Nanayakkara T, Althoefer K, Dasgupta P, et al. Soft Robotics Technologies to Address Shortcomings in Today’s Minimally Invasive Surgery: The STIFF-FLOP Approach. *Soft Robotics*. 2014;6;1(2):122-31.
- [22] Howells J. Fibre Actuator; 2024. Available from: <https://cad.onshape.com/documents/fd21cb60026f1c393fb2e134/v/4b6f37f9295e9af57b62f8ad/e/16d6a9d49bb71722a90131f9>.
- [23] Howells J. Making a PSCR Segment; 2024. Available from: <https://3-pscr.github.io/make.html>.
- [24] Micro brushless diaphragm pump;. Available from: https://www.globalsources.com/product/micro-brushless-diaphragm-pump-vacuum-pump_1164899126f.htm.
- [25] Howells J. GUI for a PSCR; 2024. Available from: <https://github.com/3-PSCR/GUI>.
- [26] Burgner-Kahrs J. Constant-Curvature Model of Tendon-driven Continuum Robots; 2022. Available from: <https://www.opencontinuumrobotics.com/101/2022/12/09/tdcr-cc-model.html>.
- [27] Lavazza J. A Study on the Mechanical Behaviour of Ecoflex 00-50 Silicone Elastomer. Milan: Politecnico Milano; 2021.
- [28] Fraš J. Instant Bending Actuator: CAD file.; 2020. Available from: https://github.com/jfras/instant_soft_robots/tree/master/bending_actuator.
- [29] Fraš J, Glowka J, Althoefer K. Instant soft robot: A simple recipe for quick and easy manufacturing. In: 2020 3rd IEEE International Conference on Soft Robotics (RoboSoft). IEEE; 2020. p. 482-8.
-]

6 Appendices

Appendix A Glossary of Terms

Term	Definition
PSCR	Pneumatic Soft Continuum Robot
Segment	One discrete section of a PSCR, with chambers that are not connected to the chambers in neighbouring segments.
Zone	Two connected chambers within a segment. Chambers in a zone are immediate neighbours, and each segment has three zones.
Lumen	The cylindrical cavity through the middle of a PSCR segment. In many robots, this is used for the routing of air hoses - in the above, it has been left clear to enable variable stiffness spines to be inserted into the robot.
Pressurisation Queue	The list of zones connected to a pump which are not yet at their target pressure, which a pump works through until the whole segment is at required pressure.
Pressure Cycle	A pre-programmed array of pressures which the robot steps through, achieving each before moving on.
Actuation	Causing a segment to bend or otherwise deform by changing the pressure supplied to it in a controlled manner.
Actuation Strategy	The algorithmic methodology used to achieve a target set of pressures in the zones of the robot.
Actuation System	Pressure control system. The pneumatic system including pumps and solenoid valves that control the actuation of the robot.
PWM Value	Value x between 0 and 255 that Arduino uses to construct a PWM signal with a duty cycle = $x/255$
Pressure Lock	Descriptive of the state when a zone's solenoid valve is closed and the segment is locked because it is at its set pressure.

Appendix B Development Work

Several ideas were trialled for aspects of the system and are not covered above.

B.1 Instant Segments

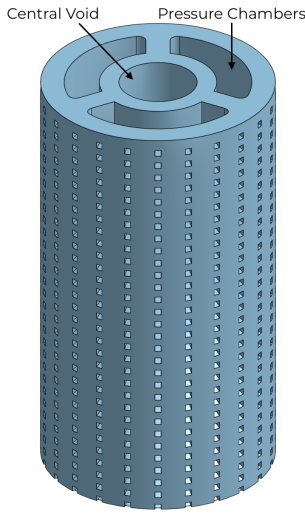


Figure 32: CAD model of the instant segment, up-scaled from J. Fraš et al.'s original [28] for new segment size.

Before a fibre-reinforced segment was selected, the first design to be tried for the segments was the Instant Soft Robot segment design (Figure 32), proposed by J. Fraš et al. [29]. It is an attractive proposition: a quick, simple way of making the reinforced body of a PSCR segment in a single silicone pour,[¶] without significant preparatory work on moulds or reinforcement. In addition, the CAD of the original design is available online. The segment uses a single-use 3D-printed mould, which has reinforcing rings built into it, arranged so that they snap off from the mould once over-moulded with silicone and then stay inside the segment (Figure 33). This structure greatly simplifies manufacture and has enormous potential for rapid prototyping of soft robotics - but, because of how the reinforcing rings are printed, it means that the air chambers in the segments have a curved-rectangle shape instead of circular cross-sections: this means they are larger relative to the segment cross-section, but also harder to reinforce effectively.

The original Instant segment was designed with an external diameter of 22 mm and an internal lumen of 4 mm. It was found to have significant problems when scaled up to the size required (35 mm OD, 13 mm lumen). This was due to two factors: the first was injection pressure, and the second print capability. The original design required that silicone be injected into the mould under pressure in order to fill all the mould

[¶]Separate pours are required for each end cap too, bringing the total to three.

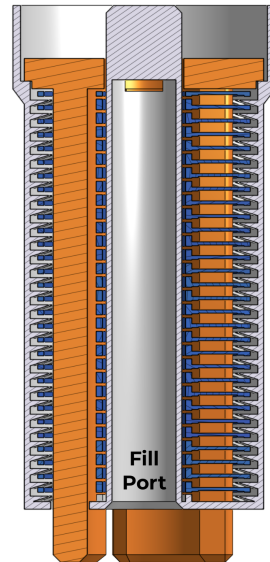


Figure 33: Cross-section of the whole mould for an instant segment - it was turned upside-down for casting, and the mould was filled through the labelled port.



Figure 34: Two Instant segments at the larger diameter - neither longer than 45 mm long, and both with significant fill issues, especially on the inside of the reinforcing rings.

cavities. With increased mould size and complexity, the pressure required was increased such that it was challenging to get the mould filled for a segment longer than around 40 mm (Figure 34). While this may have been soluble (for example by ensuring a better seal between the injector and the mouth of the mould, and between the mould parts themselves), it was found to be the less significant of the segment's problems.

The more significant of the two issues facing the larger Instant segment was printer capability. In order to break off neatly, the reinforcing rings in the mould rely on the bridging capability (ability to print without support material – Figure 35) of the 3D printing process. At a small scale, the printer is easily able to make neat bridges and keep the reinforcing rings in shape, however, as size increases this becomes problematic – the rings lack structure and become stringy,

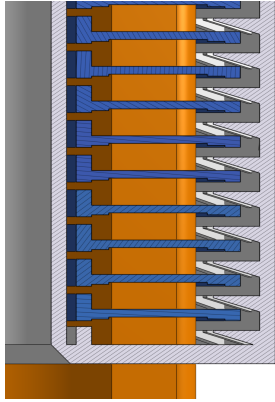


Figure 35: The moulds for the Instant segment require large spans of bridging on the reinforcement rings (blue)



Figure 36: The moulds for Instant segments relied heavily on the bridging capability of 3D printers, which was found lacking, especially at larger scales.

crossing the voids in the segment (Figure 36). This could be solved at small diameters by enabling the ‘Thick Bridges’ option in the slicer settings – but at large diameters this caused the inner part of the rings to fuse to each other, giving the segment a rigid ‘spine,’ making it unable to bend smoothly. To address these issues, it was decided that a more traditional, fibre-reinforced segment should be developed.

B.2 Piston Pump

Initially, designing a custom pump from scratch was investigated due to the cost savings this could offer. Dynamic pumps, such as centrifugal ones, were quickly rejected due to manufacturing concerns, and several types of positive displacement pumps were investigated. Bellows pumps and piston pumps emerged as frontrunners. Of the two, bellows pumps were discarded due to the difficulty of procuring bellows of suitable size and robustness. A piston design was thus investigated. Assuming a circular cross-section of piston, and with knowledge of the geometry of the segments, a relation could be derived between stroke rate n , throw T and piston diameter R :

$$V_z = 2\pi r^2 \times L \quad (= 10,780 \text{ mm}^3 \quad (3\text{s.f.}))$$

$$V_{piston} = \pi R^2 \times T$$

$$p_z V_z = 2n \times p_p V_p \rightarrow V_p = \frac{p_z V_z}{p_p \times 2n}$$

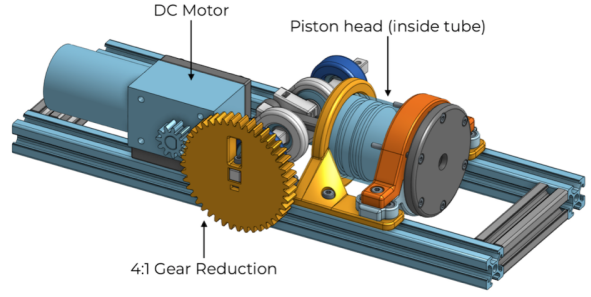


Figure 37: Annotated CAD of the piston pump (top) as well as the finished product. The main cylinder head (grey, right in the CAD) was found to leak.

$$\pi R^2 \times T = \frac{1.8 \cdot 2\pi r^2 \times L}{2n \times 1}$$

$$2n \times R^2 \times T = 3.6r^2 \times L$$

$$n \times R^2 \times T = 3087$$

where V_z , p_z and V_p , p_p are the volume and pressure of a zone (two connected chambers in a segment), and the piston respectively. r & L are the radius and length of a chamber in the segment.

Acrylic tubes were identified as a good candidate for the cylinder bore – a stock internal diameter of 47 mm was found to be practical: at a piston throw of 20 mm, it would require $n = \frac{3087}{(\frac{47}{2})^2 \times 20} = 0.279$ (3 s.f.) strokes every second, or one stroke every 3.6 seconds, in order to pressurise a zone in 2 seconds. Increasing piston throw would allow one pump to control multiple zones at once.

A piston-based pump was designed and built (Figure 37) to the above parameters and connected directly to a pressure sensor (with no check valves to control direction of air flow). It was found that the maximum pressure it could achieve was around 63 kPa (Figure 38), and a major limiting factor in this was the capability of the 3D printed parts, which were prone to bending and cracking (Figure 39). In addition, relying on 3D-printed parts (sealed using O-rings) as part of the piston and cylinder was suboptimal as the parts themselves were not airtight. Modifications to circumvent these limitations would likely have involved machining large parts of the pump system out of plastic or metal which would add significantly to the complexity. It was therefore decided that other solutions should be pursued.

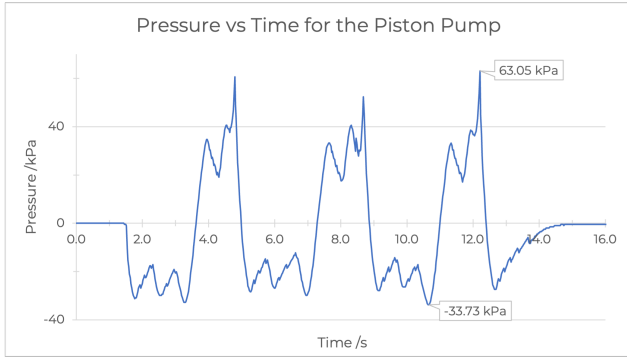


Figure 38: Maximum and minimum pressures achieved by the piston pump. Using one-way check valves to control air flow, maximum pressure could be increased to 72 kPa.



Figure 39: 3D print capability was the chief issue with the piston pump - both in terms of parts breaking and not being airtight.

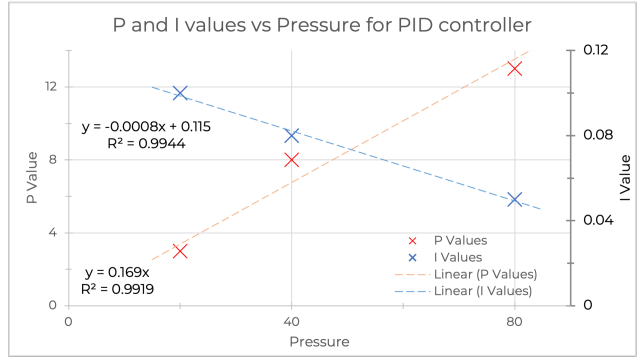


Figure 40: P and I were found to be relatively weakly correlated to pressure. However, it was found that using a more direct mapping approach to control pressure was better than PI control.



Figure 41: Pneumatic (top) vs hydraulic actuation of the same segment (before and after attachment of end caps) showing irregularities in the segment under hydraulic actuation - even at a lower curvature.

B.3 PID Control of DC Pumps

Before direct mapping was implemented to control the DC pumps, PID control was investigated. PID controllers are often used to achieve precise feedback control, so initial efforts were focused here. A simple setup was created with a pump connected directly to a segment to allow tuning of PID values. However, it became evident that straightforward PID was not the best solution: the derivative term had little to no effect, and the appropriate P and I values were found to vary based on pressure (Figure 40). Given that the segments had been found to reach a steady state for a given PWM value, a direct mapping approach was implemented instead.

B.4 Hydraulic Actuation

The segments were designed with pneumatic operation in mind – however, actuating segments with liquids such as water may have simplified control due to their incompressible nature. This was tried: one zone of a segment was filled with water, and pressure was supplied using a syringe: because water is incompressible, movement of the syringe translates directly into a change of volume of the chambers, expressed as a

bending. However, it was found that hydraulic actuation caused far more irregularities in the segment than actuation to the same bending angle by air (Figure 41). This is likely a side-effect of water’s incompressibility: once the outward pressure of the water on the ends of the segment is matched by the elastic straightening force of the segment, the water cannot be compressed, so the chambers must buckle.

Appendix C Supplementary Figures

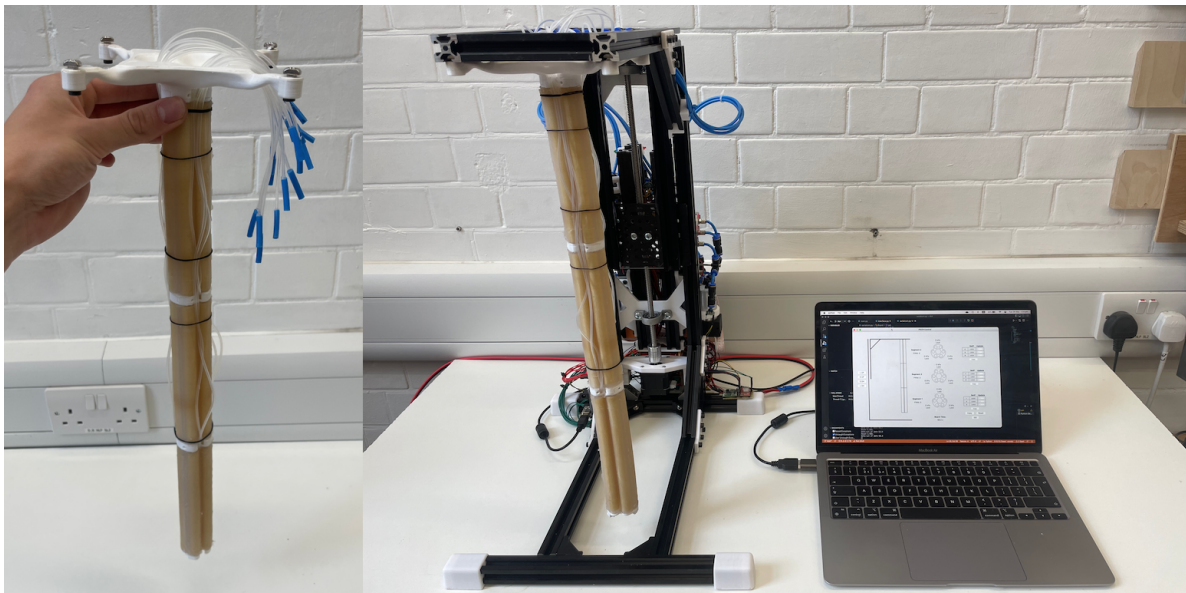


Figure 42: The three-segment arm before installation on the rig (left) and the finished rig and GUI.

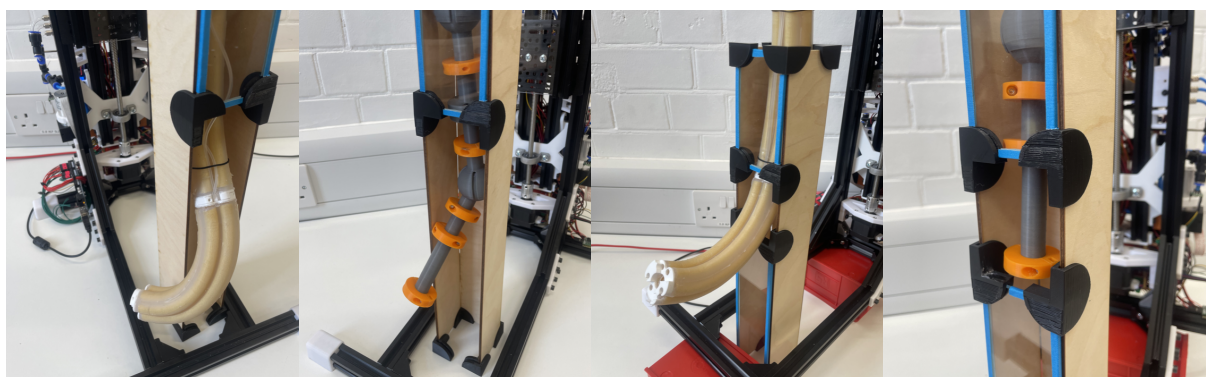


Figure 43: Comparison of soft vs rigid robot capability in navigating different obstacles.



Figure 44: A segment being removed from its mould (left), and the curvature of a Dragon Skin vs Ecoflex segment at maximum pressure (right).